Published in final edited form as:
Arch Biochem Biophys. 2013 July 1; 535(1): 56–67. doi:10.1016/j.abb.2012.12.007.

Structural and Kinetic Effects of Hypertrophic Cardiomyopathy Related Mutations R146G/Q and R163W on the Regulatory Switching Activity of Rat Cardiac Troponin I

Zhiqun Zhou[1], **Daniel Rieck**[2], **King-Lun Li**[2], **Yexin Ouyang**[1], and **Wen-Ji Dong**[1,2,*]

[1]Department of Veterinary and Comparative Anatomy Pharmacology and Physiology, Washington State University, Pullman, Washington 99164

[2]Voiland School of Chemical Engineering and Bioengineering, Washington State University, Pullman, Washington 99164

Abstract

Mutations in cardiac troponin I (cTnI) that cause hypertrophic cardiomyopathy (HCM) have been reported to change the contractility of cardiac myofilaments, but the underlying molecular mechanism remains elusive. In this study, Förster resonance energy transfer (FRET) was used to investigate the specific structural and kinetic effects that HCM related rat cTnI mutations R146G/Q and R163W exert on Ca^{2+} and myosin S1 dependent conformational transitions in rat cTn structure. Ca^{2+}-induced changes in interactions between cTnC and cTnI were individually monitored in reconstituted thin filaments using steady state and time resolved FRET, and kinetics were determined using stopped flow. R146G/Q and R163W all changed the FRET distances between cTnC and cTnI in unique and various ways. However, kinetic rates of conformational transitions induced by Ca^{2+}-dissociation were universally slowed when R146G/Q and R163W were present. Interestingly, the kinetic rates of changes in the inhibitory region of cTnI were always slower than that of the regulatory region, suggesting that the fly casting mechanism that normally underlies deactivation is preserved in spite of mutation. In situ rat myocardial fiber studies also revealed that FRET distance changes indicating mutation specific disruption of the $cTnI_{IR}$–actin interaction were consistent with increased passive tension.

Keywords

Cardiac troponin; hypertrophic cardiomyopathy; FRET; fly casting model; stopped-flow; thin filament regulation

INTRODUCTION

Hypertrophic cardiomyopathy (HCM) is characterized by ventricular hypertrophy, myofibrillar disarray, and a too often asymptomatic progression toward serious complications [1, 2]. Unfortunately, it is also one of the most common genetic

*Address correspondence to: Wen-Ji Dong, 205 Wegner Hall, Washington State University, Pullman, WA 99164. Fax: 509-335-4650; wdong@vetmed.wsu.edu.

cardiovascular diseases, with a 1:500 incidence in adults [2]. HCM is linked to dominant missense mutations in almost all of the genes encoding sarcomeric proteins, including the trimeric cardiac troponin (cTn) complex [3–5]. The goal of characterizing the pathological link between cTn mutation and HCM is thus of immense scientific importance due to the critical role that cTn plays in the Ca^{2+} dependent regulation of myocardial contractility. Comprised of subunits cardiac troponin C (cTnC), I (cTnI), and T (cTnT), cTn acts as the Ca^{2+} triggered molecular switch that controls the activation state of the thin filament. Integral to the regulatory switching function of cTn is cTnI, which itself switches from strongly interacting with actin during relaxation to strongly interacting with Ca^{2+} bound cTnC during contraction. Mutations found in human cTnI and linked to the development of HCM were first reported in 1997 and included R145G/Q, R162W, K206Q, and G203S [6]. These mutations occur in ~5% of families with HCM [7, 8]. Since 1997, more than 20 HCM-related mutations in cTnI have been reported [3, 7, 9–11].

From among the first five HCM related cTnI mutations reported in 1997 [6], R145Q, R162W, and especially R145G have received significant empirical attention. Investigations of these HCM related mutations have uncovered several mutation specific physiological effects on myocardium [3, 7, 9–11]. In the year 2000, it was demonstrated in situ by exchange of human cTnI(R145G) into porcine cardiac myofibrils that R145G reduces the extent to which human cTnI can inhibit actomyosin ATPase activity and increases the Ca^{2+} sensitivity of the myofibrillar ATPase activity profile [12]. Surprisingly, a mutation specific reduction in maximal ATPase activity was also observed, implying that R145G affects both cTnI–actin and cTnI–cTnC interactions. Similar observations were made in a later 2002 report on the effects of human cTnI(R145G) exchange into detergent skinned, porcine, left ventricular myocardial fibers, which showed decreased maximal force generation, increased passive tension, and an enhanced Ca^{2+} sensitivity and reduced steepness of force development [13]. In 2008, a very thorough investigation of the properties of skinned papillary fibers from transgenic mice bearing human cTnI(145G) largely corroborated the findings of both prior studies, but showed additionally that force per crossbridge (XB) was increased [14]. Similar observations have been made about R145Q and R162W [15]. Yet R145Q involves substitution of a positively charge arginine by glutamine which is more polar than glycine, whereas R162W involves a hydrophobic substitution at a completely different amino acid position. What mechanism could be responsible for common effects from three different mutations?

The finding that R145G/Q and R162W all affect both cTnI–actin and cTnI–cTnC interactions suggests that their mutation specific effects can be traced to their impact on the functional regions of the C-domain of cTnI (C-cTnI). It is now known that the three functional regions of C-cTnI, namely the inhibitory region ($cTnI_{IR}$), regulatory region ($cTnI_{RR}$), and mobile domain ($cTnI_{MD}$), each play a unique role in making regulatory switching possible. Each cTn regulatory switch controls one regulatory unit (RU), which in addition to one trimeric cTn consists also of one dimeric coiled-coil Tm and a seven monomer stretch of F-actin [16]. In relaxed myocardium, $cTnI_{IR}$ and $cTnI_{MD}$ bind to F-actin [17–19] and act together with tropomyosin (Tm) [20, 21] to sterically block the formation of “strong,” or force generating, actomyosin XBs within the RU [22–24]. After sarcomeric [Ca^{2+}] rises and Ca^{2+} binds to the N-domain of cTnC (N-cTnC), N-cTnC “opens” and exposes a previously buried hydrophobic pocket which binds strongly to $cTnI_{RR}$ [25, 26], sensitizing cTnC to Ca^{2+} [27, 28]. The $cTnI_{RR}$–cTnC interaction “drags” $cTnI_{IR}$ and $cTnI_{MD}$ off of actin, thus “releasing” the regulatory inhibition of strong XB formation within the RU in what is known as the “drag and release” mechanism [29–31]. This in turn causes $cTnI_{IR}$ to switch into interacting with cTnC [29], whereas $cTnI_{MD}$ becomes highly dynamic but maintains transient contacts with the thin filament [19]. Upon dissociation of Ca^{2+} from cTnC, a fly casting mechanism [32] is triggered wherein $cTnI_{MD}$ rapidly

nucleates into a binding interaction with actin, pulling $cTnI_{RR}$ out of interaction with cTnC and further pulling $cTnI_{IR}$ back down onto F-actin for inhibitory interaction [33]. Finally, should a strong XB form in the absence of Ca^{2+}, the $cTnI_{IR}$ and $cTnI_{MD}$ interactions with actin are disrupted [33–35], leaving the thin filament in a fourth "pre relax" state of regulation [36].

We have shown previously through fluorescence anisotropy measurements that each functional region of C-cTnI exhibits distinct regional protein dynamics and kinetics that play a critical role in facilitating regulatory switching [33]. R145G/Q occurs in $cTnI_{IR}$, and R162W in $cTnI_{RR}$, and all three mutations involve residue substitutions that modify amino acid side chain chemistry. For example, loss of charge resulting from R145G/Q may impact the interactions of $cTnI_{IR}$ with either actin or cTnC, whereas increased regional hydrophobicity from R162W may change the way $cTnI_{RR}$ interacts with the open hydrophobic pocket of Ca^{2+} bound N-cTnC. Furthermore, in affecting the $cTnI_{IR}$, R145G/Q may also affect $cTnI_{RR}$ which lies downstream. By the same logic, R162W may indirectly affect $cTnI_{MD}$ (or $cTnI_{IR}$ due to the fly casting mechanism) by affecting $cTnI_{RR}$. Finally, any conformational change in $cTnI_{RR}$ or impact on its conformational kinetics may be expected to affect the Ca^{2+} sensitivity of N-cTnC. It is therefore reasonable to hypothesize that changes in surface charge and hydrophobicity inherent in mutation result in mutation specific changes to regional conformation and kinetic behavior, which in turn affects regional functions essential to regulatory switching. We hypothesized further that different HCM related mutations result in similar pathology due to common mechanisms of slowing the kinetics of relaxation and changing the nature of protein-protein interactions involving predominately the $cTnI_{RR}$ and $cTnI_{IR}$.

To test our hypotheses, it would be necessary to monitor changes in the structural behavior of the functional regions of C-cTnI. Hence in this study we designed experiments to use Förster resonance energy transfer (FRET) as a spectroscopic ruler to detect mutation specific changes in distance between C-cTnI functional regions and cTnC. Recombinant single-cysteine mutant rat proteins cTnC(S89C) and either cTnI(S151C) or cTnI(S167C) were fluorescently labeled and reconstituted into thin filaments for in vitro steady state, time resolved, and stopped flow FRET measurements. This scheme is convenient because Cys-151 is positioned at the interface between $cTnI_{RR}$ and $cTnI_{IR}$, whereas Cys-167 is located at the interface between $cTnI_{RR}$ and $cTnI_{MD}$ [33]. Furthermore, it may be seen from X-ray crystal structures 1YTZ, 1YV0 [37], 11J1D and 1J1E [38] and our prior FRET studies [39, 40] that Cys-151 and Cys-167 of cTnI both experience significant Ca^{2+} dependent changes in proximity to Cys-89 of cTnC, which is located in the central linker of cTnC between its N and C domains. Thus changes in distance between Cys-89 of cTnC and Cys-151 of cTnI should reflect conformational changes involving especially the N-terminal end of $cTnI_{RR}$ and to some extent $cTnI_{IR}$, whereas Cys-167 should indicate conformational changes involving especially the C-terminal end of $cTnI_{RR}$ and to some extent $cTnI_{MD}$. To test for mutation specific effects, R146G, R146Q, or R163W (murine analogs of human HCM related mutations) were also introduced into the rat cTnI(S151C) or cTnI(S167C) construct. The major finding of our study is that R146G/Q and R163W affected C-cTnI functional region conformations uniquely, but this produced a common kinetic outcome in which $cTnI_{RR}$ and especially $cTnI_{IR}$ kinetics were slowed while leaving the fly casting mechanism itself intact. Additionally, R146Q and R163W eliminated S1-ADP dependent conformational changes usually seen in the absence of Ca^{2+}, strongly indicating a mutation-specific disruption of the $cTnI_{IR}$–actin interaction that resembles the fourth pre-relax state of thin filament regulation. These observations directly explained the pathophysiological outcomes of these mutations which were verified in situ in detergent skinned myocardial fibers from rat.

MATERIALS AND METHODS

Protein sample preparation and characterization

To implement FRET in this study, a series of recombinant single-cysteine mutants were generated from wild type rat protein clones using approaches similar to those previously reported [41]. The mutants generated included: cTnI(S151C), cTnI(S167C), cTnC(S89C), cTnI(S151C/R146G), cTnI(S151C/R146Q), cTnI(S151C/R163W), cTnI(S167C/R146G), cTnI(S167C/R146Q) and cTnI(S167C/R163W). Note that in these mutants, endogenous cysteine residues Cys-35 and Cys-84 in cTnC have been substituted with serines [25] and Cys-81 and Cys-98 in cTnI have been substituted with serine and isoleucine, respectively [42]. Furthermore, the substitutions R146G/Q and R163W were used in our rat proteins to mimic the HCM related mutations R145G/Q and R162W found in human cTnI. All cTnI proteins were purified and modified with 5-((((2-Iodoacetyl)amino)ethyl)amino)Naphthalene-1-Sulfonic Acid (AEDANS) as FRET donor according to previously described procedures [25, 43]. cTnC(S89C) was purified and labeled with N-(4-Dimethylamino-3,5-dinitrophenyl)maleimide (DDPM) as FRET acceptor by following a previously described procedure [29] to produce cTnC($S89C_{DDPM}$). The labeling ratio was determined spectroscopically using $\varepsilon_{325\ nm}$ = 6,000 $cm^{-1}{\cdot}M^{-1}$ for AEDANS and $\varepsilon_{442\ nm}$ = 2930 $cm^{-1}{\cdot}M^{-1}$ for DDPM. Labeling ratios for all protein modification were >95%. Recombinant wild-type rat cTnT was purified as previously reported [25]. cTm and S1 from the chymotryptic digestion of myosin were obtained from bovine cardiac tissue [44, 45]. Actin was purified from rabbit skeletal muscle [46]. Single-cysteine cTnC and cTnI mutants were reconstituted into thin filament samples using a cTn : Tm : actin molar ratio of 1 μM : 1 : 7.5 and checked by Native Gel as previously reported [33, 39]. The biochemical activity of the labeled cTnI and cTnC mutants, used before in our laboratory, was also verified by Ca^{2+}-dependent regulation of acto-S1 ATPase activity [39] (data not shown). Multiple experiments were performed on the samples prepared within 2 weeks, and no protein degradation was observed during electrophoretic analysis.

Steady-state in vitro measurements of emission spectra and the Ca^{2+}-dependence of regulatory switching

Proper labeling of single-cysteine cTnC and cTnI mutants and FRET efficacy were first verified using steady-state measurements of AEDENS (donor) emission spectra carried out at 10 ± 0.1°C on an ISS PCI photon-counting spectrofluorometer equipped with a micro titrator [25]. Single-cysteine cTnC and cTnI mutants were reconstituted into thin filaments as follows. Donor-acceptor samples were prepared containing the desired S151C-bearing cTnI mutant labeled with AEDENS and cTnC(S89C) labeled with DDPM. Donor only samples were prepared as controls, and contained the desired S151C-bearing, AEDENS-labeled cTnI mutant and cTnC(wt) instead of cTnC(S89C). Samples were made up to 1.2 mL in a titration solution containing (in mM): 40 3-(N-morpholino)propanesulfonic acid (MOPS, pH 7.0), 2 ethylene glycol tetraacetic acid (EGTA), 150 KCl, 5 $MgCl_2$, and 1 DTT. Spectra were then determined in the absence and presence of acceptor under the following four biochemical conditions: 1) Ca^{2+} absent, 2) 2 mM Ca^{2+} present, 3) Ca^{2+} absent and 5 μM S1-ADP present, 4) 2 mM Ca^{2+} plus 5 μM S1-ADP present. Samples were illuminated with 343 nm excitation light, and the fluorescence intensity of the AEDANS emission was monitored at 480 nm.

To determine the mutation-specific effects on the Ca^{2+}-dependence of regulatory switching, steady-state in vitro fluorescence measurements were then taken over the course of Ca^{2+} titrations carried out using the micro titrator as described previously [40]. Briefly, Ca^{2+}-titrations were designed to reveal the Ca^{2+} dependence of regulatory switching as indicated by changes in distance between either 1) Cys-89 of cTnC and Cys-151 of cTnI, or 2) Cys-89

of cTnC and Cys-167 of cTnI. In a typical titration experiment, up to 100 data points were acquired after successively injecting aliquots of 3 μL of a high [Ca^{2+}] buffer. Data from Ca^{2+}-titrations were fit using the Hill equation:

$$I = (I_{max} - I_{min}) \frac{\left[Ca^{2+}\right]^{n_H}}{\left[Ca^{2+}\right]^{n_H} + \left(10^{-pCa_{50}}\right)^{n_H}} + I_{min} \quad (1)$$

where I represents steady state AEDENS intensity, I_{max} AEDENS intensity under Ca^{2+} saturated conditions, I_{min} AEDENS intensity under Ca^{2+} free conditions, pCa_{50} the $-Log_{10}([Ca^{2+}])$ at which apparent half-occupancy of N-cTnC Ca^{2+} binding sites occurs, and n_H the Hill coefficient or steepness of the Ca^{2+} dependent reduction in AEDENS fluorescence.

Determining mutation-specific changes in cTnI-to-cTnC FRET distances using fluorescence lifetime measurements

To accurately determine distance changes associated with mutation-specific changes to the regional C-cTnI conformations associated with regulatory switching, fluorescence intensity decays were measured in the time domain using a FluoroCube (HORIBA Jobin Yvon) lifetime system with an L-format detection arrangement. Using the same biochemical conditions as those used to determine AEDENS emission spectra, lifetime decays were obtained for each sample under each biochemical condition. Decays were recorded with TBX picosecond photon detection modules and fitted with a multi exponential function [47]:

$$I(t) = I_0 \sum_i \alpha_i \cdot e^{-t \cdot \tau_i^{-1}} \quad (2)$$

where the α_i represents the fractional amplitude associated with each correlation time τ_i contributing to the overall lifetime decay. The best fit α_i and τ_i from Eqn. 2 for a sample under a certain biochemical condition were then used to calculate the average lifetime $\bar{\tau}$ for that sample from the equation:

$$\bar{\tau} = \sum_i \alpha_i \cdot \tau_i \quad (3)$$

The FRET efficiency for each combination of sample and biochemical condition was then calculated by the following relationship:

$$E = 1 - \frac{\bar{\tau}_{DA}}{\bar{\tau}_D} \quad (4)$$

Where $\bar{\tau}_{DA}$ represents the average lifetime of the donor-acceptor test sample and $\bar{\tau}_D$ the matching donor-only control sample under the biochemical condition tested. The statistical significance of differences in energy transfer efficiency was determined using a two tailed Student's t test.

In vitro stopped-flow measurements

Fluorescence intensity measurements taken during stopped-flow were used to examine the kinetics describing changes in the distances between C-cTnI and N-cTnC as induced by Ca^{2+} dissociation. Experiments were performed with a T format KinTek stopped flow spectrometer with a 1.8 ms dead time. Ca^{2+}-saturated, reconstituted thin filament samples were rapidly mixed with an equal volume of buffer containing an excess amount of the Ca^{2+}

chelator 1,2-bis(2-aminophenoxy)ethane-*N,N,N′,N′*-tetraacetic acid (BAPTA) [48]. As in equilibrium FRET experiments, the time-dependent change in AEDANS emission intensity was first determined for a donor only sample, followed by determination of the time dependent emission intensity for the corresponding donor-acceptor sample. A total of 8–10 kinetic traces were collected for each set of donor only and donor-acceptor samples. The set of kinetic traces for each sample was averaged and then nonlinear regression was used to fit the averaged trace with a monoexponential and determine the rate of conformational change.

Exchange of troponin with recombinant rat cTnI mutations into detergent-skinned rat cardiac muscle fiber bundles

The method followed for preparing rat cardiac muscle fibers and the solutions used for testing them are based on the protocols described by the Chandra laboratory [49]. Briefly, left ventricular papillary fiber bundles were dissected from male Long-Evans rats, aged 6–7 months, in relaxing solution containing (in mM): 50 N,N-bis (2-hydroxyethyl)-2-amino-ethane-sulfonic acid (BES, pH 7.0), 30.83 K^+ propionate, 20 2,3-butanedione monoxime (BDM), 20 EGTA, 6.29 MgCl2, 6.09 Na_2ATP, 5 Na azide, and 1.0 DTT. A cocktail of fresh protease inhibitors (4 μM benzamidine-HCl, 5 μM bestatin, 2 μM E-64, 10 μM leupeptin, 1 μM pepstatin and 200 μM phenylmethylsulfonyl fluoride) were added to all buffered solutions. Smaller muscle “fibers” (~150–200 μm in diameter and ~2.0 mm in length) were dissected from fiber bundles and then skinned overnight using 1% triton X-100 in relaxing solution at 4 °C. Endogenous cTn was exchanged for exogenous recombinant cTn by equilibrium. Trimeric cTn complexes were first reconstituted to a ~20 μM concentration from the desired single cysteine cTnI mutant, cTnC(wt) and cTnT(wt) proteins. Reconstituted cTn complexes were then dialyzed into an exchange buffer containing (in mM): 200 KCl, 5 MgCl2, 5 EGTA, 20 MOPS pH 6.5, and 1 DTT. Detergent skinned muscle fibers were then incubated with the reconstituted cTn complexes in exchange buffer overnight at 4 °C based on the method of the de Tombe laboratory [50]. To quantify exchange, recombinant cTn complexes containing N-terminal c-Myc-tagged mouse cTnT were also used in combination with Western blotting with antibody against cTnT [51].

In situ Determination of mutation specific effects on force-Ca^{2+} relationships

After recombinant cTn complexes had been exchanged into muscle fibers, the strips were mounted in a Güth Muscle Research System [52]. Fibers were mounted on two stainless steel tweezers and inserted into the optical cuvette of the apparatus filled with relaxing solution, with one tweezers serving as the pin of an optical force transducer. The cuvette consists of a 1 cm long quartz capillary with an inner diameter of 1 mm. The sarcomere length of the fibers was set to 2.2 μm using a laser diffraction pattern. The cross sectional area of each fiber was calculated from images captured using a Moticam 2000 microscope camera. Motic Images Plus software was used to process images, and calculations assumed that the fibers were elliptical prisms. To determine the force-Ca^{2+} relationship of tested fibers, fiber stress was measured in response to a series of titration solutions with pCa values ranging from 9 to 4.3. The composition of the final titration solution with pCa = 4.3 was as follows (in mM): 10 EGTA, 10.11 $CaCl_2$, 6.61 $MgCl_2$, 5.95 Na_2ATP, 30.83 K^+ propionate, and a cocktail of protease inhibitors. The initial titration solution with pCa = 9.0 was of the same composition with the following exceptions (in mM): 0.0242 $CaCl_2$, 6.87 $MgCl_2$, 5.83 Na_2ATP, and 51.14 potassium propionate. These titration solution compositions were determined using pCa Calculator [53]. Finally, the averaged force-Ca^{2+} relationship for each fiber type was fitted to a Hill equation describing the force-Ca^{2+} relationship of the following form:

$$S = (S_{max} - S_{min}) \frac{\left[Ca^{2+}\right]^{n_H}}{\left[Ca^{2+}\right]^{n_H} + \left(10^{-pCa_{50}}\right)^{n_H}} + S_{min} \quad (5)$$

where S_{max} represents maximal stress under Ca^{2+} saturated conditions, S_{min} the passive stress under relaxing conditions, n_H the Hill coefficient, and pCa_{50} the pCa value producing half occupancy of Ca^{2+}-binding sites and thus half maximal stress. Parameter values were compared based on a two tailed Student's t test.

RESULTS

R146G/Q and R163W increase the Ca^{2+}-sensitivity of conformational transitions involving the C-domain of cTnI

The broad experimental goal of our study was to use FRET to determine the mutation specific effects of R146G/Q and R163W on the conformational transitions that C-cTnI undergoes during regulatory switching. It was therefore critical at the start of investigation to establish two essential points. Firstly, the efficacy of our FRET scheme should be verified in the context of this new experimental effort. Secondly, it should be confirmed that R146G/Q and R163W function as murine analogs of the human HCM related mutations, at least at the in vitro level. So in order to verify proper fluorophore labeling and FRET efficacy once our recombinant proteins were incorporated into reconstituted thin filaments, AEDENS emission spectra from our samples were measured under several biochemical conditions.

Fig. 1 demonstrates comprehensively that FRET occurs as expected between AEDENS labeled cTnI(S151C) (cTnI($S151C_{AEDENS}$)) and cTnC($S89C_{DDPM}$) in the reconstituted thin filament. A donor only sample containing cTnI($S151C_{AEDENS}$) and cTnC(wt) established a baseline emission spectrum for AEDENS, and this spectrum was found to be insensitive to changes in Ca^{2+} or the introduction of S1-ADP (data not shown). With Ca^{2+} and S1-ADP absent, a reduction in AEDENS spectral intensity was observed when cTnC($S89C_{DDPM}$) replaced cTnC(wt), demonstrating a basal level of FRET taking place between AEDENS and DDPM. Introduction of Ca^{2+} and S1-ADP further reduced the AEDENS spectral intensity, indicating increased FRET. This made sense, because Cys-151 of cTnI was expected to move closer to Cys-89 of cTnC since Ca^{2+} binding causes localization between $cTnI_{RR}$ and N-cTnC and induces the $cTnI_{IR}$ to switch from interacting with actin to interacting with cTnC. Furthermore, S1 is known to be capable of moving Tm to the open position in the absence of Ca^{2+}, which disrupts C-cTnI–actin interactions [33] and produces a fourth pre-relax state of thin filament regulation [36]. Trends were very similar for samples containing cTnI($167C_{AEDENS}$) instead of cTnI($151C_{AEDENS}$) (data not shown).

Having verified the efficacy of our FRET scheme, next we turned toward characterizing the effects of R146G/Q and R163W on the Ca^{2+} dependence of the C-cTnI conformational transitions involved in regulatory switching. Increased Ca^{2+}-sensitivity is a hallmark of HCM related mutations. Thus we performed Ca^{2+} titrations on our reconstituted thin filament samples, expecting to see mutation specific increases in pCa_{50} (see Eqn. 1). Fig. 2A shows through traces of the Ca^{2+} dependence of changes in FRET efficiency observed in samples containing cTnC($S89C_{DDPM}$) and single cysteine cTnI mutants containing $S151C_{AEDENS}$ that R146G/Q and R163W all increased the pCa_{50} relative to control. Furthermore, there was generally a leftward (i.e. more Ca^{2+} sensitive) shift of each trace due to the presence of S1 (Fig. 2B). As with changes in AEDENS spectral intensity, trends were very similar for samples containing cTnI($167C_{AEDENS}$) instead of cTnI($151C_{AEDENS}$) (data not shown).

Table 1 shows the results of nonlinear regression of Eq. 1 to fit the traces shown in Fig. 2. Control samples responded to Ca^{2+} and S1-ADP as expected. Reconstituted thin filaments containing cTnC(S151C_{AEDENS}) behaved similarly as filaments cTnC(S167C_{AEDENS}) in terms of the Ca^{2+}-sensitivity and steepness of Ca^{2+}-dependent changes in FRET efficiency. S1-ADP also produced the expected increase in pCa_{50} and decrease in n_H for these samples. S1-ADP should move cTm to the open position, thereby disrupting interactions between actin and C-cTnI. This allows a partial interaction between cTnC and $cTnI_{RR}$ that sensitizes N-cTnC to Ca^{2+} and increases the pCa_{50}. Cooperativity also depends on coupling between RUs that is facilitated by cTm (ref). By forcing cTm to the open position throughout the filament, S1-ADP reduces the potential for further purely Ca^{2+}-dependent allosteric interaction between RUs, thereby decreasing n_H. Having obtained these expected trends, we could reliably compare the behavior of control samples versus samples containing HCM mutations to elucidate their mutation specific effects on TF regulation and the regulatory function of C-cTnI.

Regarding mutation specific effects on the Ca^{2+}-sensitivity of TF activation, the largest increase in pCa_{50} was seen from R163W followed closely by R146G when considering changes in distances from both Cys-151 and Cys-167 of cTnI to Cys-89 of cTnC. This made sense, as the replacement of the positively charged, salt bridging, and amphipathic side chain of arginine with a hydrophobic side chain could drastically change and possibly enhance the nature of the interaction between the $cTnI_{RR}$ and N-cTnC. R146G replaces the side chain of arginine with a small hydrogen atom, which may weaken $cTnI_{IR}$ interactions by a loss of former side chain chemistry that does not involve added and prohibitive chemical constraints. R146Q gave the smallest increase in pCa_{50}, which was about half that of R163W when considering the overall increase in the pCa_{50} (i.e. for both S151C_{AEDENS} and S167C_{AEDENS} containing samples). R146Q involves the replacement of arginine with glutamine, whose polarity should drive it to the protein surface and into exposure to the aqueous environment of solvent; this may produce a significantly deleterious impact to $cTnI_{IR}$ interactions.

It is therefore notable that in the presence of R146Q and R146G, the impact of S1-ADP on the overall pCa_{50} of regulatory switching was attenuated relative to control. This may suggest that R146Q and R146G destabilize the blocked state such that TF activation is “partially triggered” even in the absence of Ca^{2+}. In this case, in moving cTm to the open state independent of Ca^{2+}, S1-ADP would not produce as drastic an effect on Ca^{2+}-dependent behavior. This suggests that these HCM related mutations may cause the TF to enter something like the pre relax state independent of S1-ADP. The situation may be somewhat different for R163W, which likely enhances the strength of interaction between $cTnI_{RR}$ and N-cTnC. This could potentiate the purely S1-ADP dependent effects on the Ca^{2+}-sensitivity of activation even if C-cTnC–actin interactions are disrupted. Nevertheless, if R146G/Q and R163W cause the TF to mimic the pre relax state in the absence of S1-ADP, one might expect reduced TF cooperativity.

Mutation specific changes in the steepness of TF activation were indeed consistent with changes in Ca^{2+} sensitivity. Table 1 shows that the tested mutations tended to reduce the n_H of Ca^{2+} dependent changes in FRET efficiency. R163W produced the largest overall decrease in n_H relative to control, similar to its large effect on pCa_{50}. R146G and R146Q reduced n_H by a similar amount. These reductions in n_H are also reminiscent of the effect of S1-ADP on TF activation, just as trends in pCa_{50} suggested. Supporting this notion, the impact of S1-ADP on n_H was generally attenuated in the presence of mutation. Overall, the mutation-specific effects of R146G/Q and R163W on regulatory switching were thus consistent with expectations while already suggesting that changes to regulatory switching unique to each mutation may lead to similar behavioral outcomes. Particularly, HCM related

mutations seemed to cause the TF to enter a pre relax like TF state in the absence of S1-ADP.

R146G/Q and R163W each uniquely affect the C-cTnI conformational transitions underlying regulatory switching

Having verified our experimental approach and seen different but expected mutation specific increases in the Ca^{2+} sensitivity of Ca^{2+} dependent C-cTnI conformational transitions, it was time to apply FRET as a spectroscopic ruler to determine the precise structural effects of R146G/Q and R163W on C-cTnI during regulatory switching. Would it be possible to illuminate the currently observed effects of these mutations on thin filament regulation based on how they structurally impact the $cTnI_{RR}$, $cTnI_{IR}$, and $cTnI_{MD}$? To answer this question, time-resolved fluorescence measurements were performed to obtain AEDENS fluorescence lifetimes that could be used to precisely determine changes in FRET efficiency. With a sixth-power dependence on intra-fluorophore distance, FRET efficiency is a powerful measure of changes in molecular structure involving relative spatial displacement. Fig. 3A shows a series of representative AEDENS emission intensity decays observed under different biochemical conditions in thin filaments reconstituted with either cTnC(wt) or cTnC($S89C_{DDPM}$) and either cTnI($S151C_{AEDENS}$) or cTnI($S151C_{AEDENS}$/R146G). The trends observed in these decays were consistent with the measurements of AEDENS emission spectral intensities shown in Fig. 1. AEDENS intensity decays from donor-only samples were insensitive to the addition of Ca^{2+}. When acceptor was present, the decay became faster and the fluorescence lifetime was decreased, indicating FRET between AEDENS and DDPM. Finally, FRET efficiency was clearly increased by both the addition of Ca^{2+} and the addition of S1-ADP, both of which should increase the proximity between AEDENS and DDPM in this case.

Quantitatively speaking, intensity decays were well described by a two exponential function (see Eqn. 2), which suggested that the overall donor lifetime could be resolved from the combined effect of a faster and a slower decay process. Fluorescence lifetimes and FRET efficiencies were thus determined from AEDENS emission intensity decays using Eqns. 2–4 and nonlinear regression, and are shown in Table 2. Fig. 3B is a chart of biochemically induced changes in FRET efficiency between $S151C_{AEDENS}$ of cTnI and $S89C_{DDPM}$ of cTnC, and Fig. 3C shows the results for $S167C_{AEDENS}$ of cTnI. To facilitate a clear analysis of the data, we shall denote the distance between $S151C_{AEDENS}$ of cTnI and $S89C_{DDPM}$ of cTnC as the “151C↔89C” distance. Likewise, the distance between $S167C_{AEDENS}$ of cTnI and $S89C_{DDPM}$ of cTnC shall be termed the “167C↔89C” distance. Furthermore, mutation-specific effects will be inspected in two ways. Firstly, mutation-specific changes in 151C↔89C and 167C↔89C distances at each biochemical condition will be considered. Table 2 is more representative of this kind of information. Secondly, the way that mutations affect the magnitude and direction (i.e. positive or negative) that 151C↔89C and 167C↔89C distances change when transitioning from one biochemical condition to another will also be considered. In this latter case, Fig. 3B–C present this type of information most clearly. Note that unless otherwise indicated in the text or in the footnotes of Tables 2 and 3, all reported differences in FRET efficiency are statistically significant. Overall, considerable structural information is presented in Table 2 and Fig. 3; but it is immediately and intuitively obvious that R146G/Q and R163W each affect the structure of the $cTnI_{RR}$ and likely the $cTnI_{IR}$ and $cTnI_{MD}$ differently.

Let us first consider the biochemical state transition from $Mg^{2+} \rightarrow Ca^{2+}$, which represents thin filament regulatory switching in the absence of XB cycling. Looking at the Mg^{2+} state (Tables 2 and 3, “Thin filament + Mg^{2+}” sample group), R146G/Q and R163W all tended to increase the 151C↔89C distance and decrease the 167C↔89C distance relative to control (i.e. no HCM-related mutation present), with R146G producing the largest changes in FRET

efficiency. Looking at the Ca^{2+} state, R146G and R163W tended to increase the 151C↔89C distance (Table 2, "Thin filament + Ca^{2+}"). Relative to control, this led to R146G/Q and R163W specific increases in the distance traversed by Cys-151 of cTnI in moving toward Cys-89 of cTnC when the thin filament transitioned from the Mg^{2+} state to the Ca^{2+} state (Fig. 3B, "$Mg^{2+} \rightarrow Ca^{2+}$" sample group). Regarding the 167C↔89C distance in the Ca^{2+} state relative to control (Table 3, "Thin filament + Ca^{2+}"), R146G decreased it, whereas both R146Q and R163W increased it. Relative to control, this led to R146G/Q and R163W specific decreases in the distance traversed by 167C in moving toward 89C when the thin filament transitions from the Mg^{2+} state to the Ca^{2+} state (Fig. 3C, "$Mg^{2+} \rightarrow Ca^{2+}$"). These structural differences amount to distinct modes of interfering with the usual regulatory switching mechanism intrinsic to the thin filament.

Considering each mutation separately, changes in FRET efficiency suggested that R146G produces an overall tighter localization between $cTnI_{RR}$ and N-cTnC in the Ca^{2+} state, since it increased both the 151C↔89C and 167C↔89C proximities relative to control. This implied that R146G enhances the $cTnI_{RR}$–cTnC interaction in the Ca^{2+} state, which should produce a greater sensitization of N-cTnC to Ca^{2+}. As mentioned above, R146G also increases the proximity of the $cTnI_{RR}$ and N-cTnC in the Mg^{2+} state (Table 3, "Thin filament + Mg^{2+}"). This suggests that R146G disrupted the $cTnI_{IR}$–actin interaction allowing $cTnI_{RR}$ to move closer to N-cTnC in the Mg^{2+} state. Since the 167C↔89C distance changed and Cys-167 of cTnI is adjacent to the $cTnI_{MD}$, there is also the potential for a long distance impact on the $cTnI_{MD}$–actin interaction but this is less clear from the data. Using this logic, R146Q appeared to disrupt both the $cTnI_{IR}$–actin interaction in the Mg^{2+} state and the $cTnI_{RR}$–cTnC interaction in the Ca^{2+} state. Firstly, it increased the 167C↔89C FRET distance in the Mg^{2+} state (Table 3, "Thin filament + Mg^{2+}"). Secondly, it reduced the 167C↔89C FRET efficiency by 6.37% in the Ca^{2+} state (Table 3, "Thin filament + Ca^{2+}") relative to control, while leaving the 151C↔89C distance unchanged (Table 2). Finally, R163W appeared to significantly disrupt the $cTnI_{IR}$–actin interaction and also affect the $cTnI_{RR}$–cTnC interaction. R163W increased the proximity of the $cTnI_{RR}$ and N-cTnC in the Mg^{2+} state (Table 3, "Thin filament + Mg^{2+}"), and increased the 151C↔89C proximity in the Ca^{2+} state (Table 2, "Thin filament + Ca^{2+}"). Curiously, R163W also reduced the 167C↔89C proximity in the Ca^{2+} state relative to control (Table 3, "Thin filament + Ca^{2+}"). However, it was unclear whether this represented a pulling of the C-terminal end of the $cTnI_{RR}$ away from N-cTnC, or instead a tighter localization between the C-terminal end of the $cTnI_{RR}$ with a region of N-cTnC further away from Cys-89C of cTnC.

Since R146G/Q and R163W affect regulatory switching in the absence of strong XBs, what then happens when the XB cycle comes into the molecular picture? To address this question, the biochemical state transition from $Mg^{2+} \rightarrow Mg^{2+}$ + S1-ADP was first considered. In this case, the thin filament is transitioning from the blocked state to the pre relax state [33, 36] of regulation. This transition would be expected to occur either when sarcomeric [Ca^{2+}] is at the relaxing level but strong XBs nevertheless form within the RU (e.g. possible during ischemia [54, 55]), or when during the process of myocardial relaxation Ca^{2+} dissociates from N-cTnC before any XBs within the RU detach. Under normal circumstances, one would expect S1-ADP mediated disruption of the $cTnI_{IR}$–actin interaction and a concomitant increase in the proximity between $cTnI_{RR}$ and actin. This is seen in the controls as both the 151C↔89C and 167C↔89C distances decreased due to the presence of S1-ADP (Tables 2 and 3, "Thin filament + S1-ADP + Mg^{2+}"). Interestingly, the S1-ADP dependent increase in 151C↔89C proximity disappeared when R146G/Q and R163W were present, strongly suggesting that the $cTnI_{IR}$–actin interaction was already disrupted due to the mutations such that S1-ADP produced no statistically significant effect. Since the role of the $cTnI_{MD}$ in the absence of Ca^{2+} and S1-ADP is to stabilize the $cTnI_{IR}$–actin interaction, now disrupted, it is also possible the $cTnI_{MD}$–actin interaction was also impacted by mutation.

For R146G/Q, the addition of S1-ADP did significantly increase the 167C↔89C proximity, whereas no S1-ADP dependent statistically significant increase in the 167C↔89C proximity was seen for R163W. Thus consistent with our titration data in Table 1, the determined FRET efficiencies strongly suggested that in the absence of Ca^{2+} and the presence of R146G/Q and especially R163W, the thin filament is shifted into a hybrid conformational state somewhere in between the blocked state and the pre relax state.

Another important effect of strong XBs (i.e. S1-ADP) is their role in promoting the sensitization of N-cTnC to Ca^{2+}, which has been observed in numerous studies [56, 57] and is a critical aspect of the pre relax state [36]. One would thus expect to observe a tighter localization between $cTnI_{RR}$ and N-cTnC during the $Ca^{2+} \rightarrow Ca^{2+}$ + S1-ADP state transition. This is indeed observed in Table 3 ("Thin filament + Ca^{2+}" versus "Thin filament + S1-ADP + Ca^{2+}") with mutation absent, though the 151C↔89C distance in table 2 did not change significantly. However, R146Q and R163W surprisingly resulted in a S1-ADP dependent increase in the 151C↔89C distance when S1-ADP was added with Ca^{2+} present (Fig. 3B, "$Ca^{2+} \rightarrow Ca^{2+}$ + S1"). In the case of R146Q, both the 151C↔89C and the 167C↔89C proximities were less compared to control in the Ca^{2+} + S1-ADP state. Nevertheless, with R146Q and Ca^{2+} present S1-ADP increased the mean 167C↔89C FRET efficiency by 4.38%, which is over double the magnitude of the aforementioned S1-ADP dependent decrease in the 151C↔89C FRET efficiency. This suggested that S1 helps to restore the overall localization between the $cTnI_{RR}$ and N-cTnC with R146Q and Ca^{2+} present. In the case of R163W, regulatory switching appeared to be so affected by mutation that S1-ADP not only produced no apparent structural effects on $cTnI_{RR}$ with Ca^{2+} absent, but also produced no effect when Ca^{2+} was present. Thus the detailed structural information provided in our time-resolved measurements of FRET strongly suggested that the different effects of R146G/Q and R163W on C-cTnI regulatory switching were caused by unique impacts on the steady state structural and functional behavior of $cTnI_{IR}$ and $cTnI_{RR}$, and possibly $cTnI_{MD}$. But how might these mutation-specific effects seen in steady-state experiments impact the dynamic behavior of the cardiomyocyte?

The kinetics of thin filament deactivation are slowed by R146G/Q and R163W

To investigate the potential for effects from R146G/Q and R163W on the kinetics of regulatory switching and thus the dynamics of myocardial contractility, stopped-flow experiments were performed. This step was also important for corroborating insights from steady state structural information. Since Ca^{2+}-dependent equilibria between C-cTnI conformational states arises from a kinetic balance, then the structural changes that cause the mutation specific effects seen under steady state conditions should also produce changes in kinetics. Furthermore, the information gathered at this point of the study had most directly assessed the effects of mutation on the function of the $cTnI_{RR}$, since Cys-151 and Cys-167C of cTnI are located at either end of the $cTnI_{RR}$. Insights gained from 151C↔89C FRET distances about impacts of especially R146G/Q and also R163W on $cTnI_{IR}$ function can be corroborated by prior literature that documents mutation specific effects on passive tension development or the inhibition of actomyosin ATPase activity. But what about what 167C↔89C distances suggest about the function of the $cTnI_{MD}$, a region relatively distant from the points of mutation? Since $cTnI_{MD}$ catalyzes the deactivation of the thin filament, kinetic information might reveal mutation specific long distance effects on $cTnI_{MD}$ structural behavior that were not evident under steady state conditions.

Fig. 4 shows a series of averaged traces of increases in AEDENS emission intensity due to Ca^{2+} dissociation observed in thin filaments reconstituted with cTnC($S89C_{DDPM}$) and single cysteine cTnI mutants containing $S151C_{AEDENS}$. Figs. 4A and 4B show kinetic traces collected in the absence or presence of S1, respectively. Table 4 shows the results of fitting monoexponentials to the traces presented in Fig. 4, as well as traces collected from thin

filaments reconstituted with cTnC($S89C_{DDPM}$) and single cysteine cTnI mutants containing $S167C_{AEDENS}$. Control samples gave results consistent with a prior FRET study from our lab [40] where it was observed that the kinetics of regional conformational changes involving Cys-167 of cTnI are more rapid than changes involving Cys-151 of cTnI. This suggested that conformational changes in C-cTnI occur more rapidly as one nears the N-terminus, which is reminiscent of the fly casting model [32]. This was later confirmed by fluorescence anisotropy measurements [33] that clearly showed that kinetic rates describing conformational changes in C-cTnI functional regions are ranked $cTnI_{MD} > cTnI_{RR} > cTnI_{IR}$, validating the fly casting model in thin filaments. Addition of S1-ADP universally slowed the action of the mechanism while preserving the ranking of kinetic rates in both studies, and this was seen again in the current study. What is most fascinating is that R146G/Q and R163W largely produced kinetic effects similar to that of S1-ADP in the absence of mutation.

Relative to control, all the mutations slowed the apparent kinetics of the $cTnI_{RR}$ and $cTnI_{IR}$ as reflected by changes in the 151C↔89C distance. Mutation specific changes in the 167C↔89C distance suggested that changes in $cTnI_{MD}$ conformation were also slowed by R146G and R163W, but made faster by R146Q. None of the mutations changed the $cTnI_{MD} > cTnI_{RR} > cTnI_{IR}$ ordering of kinetic rates, suggesting that all the molecular mechanisms encapsulated in the fly casting model (which we will hereafter term “the fly casting mechanism”) still functioned on some level in spite of mutation. This is summarized in Scheme 1. Interestingly, the slowing effect of S1-ADP on $cTnI_{IR}$ conformational transitions was attenuated by all three mutations as suggested by changes in the 151C↔89C distance. This attenuation was generally not as severe for changes in the C-terminal portion of $cTnI_{RR}$ and the N-terminal portion of $cTnI_{MD}$ as indicated by changes in 167C↔89C proximity. In fact, S1-ADP had a greater slowing effect for samples containing R146Q relative to control. This suggested that R146Q disrupts the $cTnI_{RR}$–cTnC interaction, allowing the nucleation of $cTnI_{MD}$ onto actin to pull the $cTnI_{RR}$ away from cTnC more rapidly. This agreed well with the much lower extent of Ca^{2+} sensitization seen in our titration data (Table 1). However, R146Q also seems to disrupt the $cTnI_{IR}$–actin interaction, such that the rate of the return of $cTnI_{IR}$ to actin is not statistically different than in the case of control with S1-ADP present (Table 4, 151C/R146Q, $p > 0.10$). In other words, our combined data suggests that R146Q dampens regulatory switching while also preventing the complete return of Tm to the blocked state, leaving the TF in a pre relax like state.

Given the interpretation that the slower kinetics seen with R146Q implied dampened regulatory switching, what then is the significance of the even slower rate of return of $cTnI_{IR}$ to actin seen when R146G was present? In the case of R146G, the $cTnI_{RR}$–cTnC interaction was suggested to be enhanced by our prior data sets, implying that nucleation of $cTnI_{MD}$ onto actin was less effective at pulling $cTnI_{RR}$ and especially the $cTnI_{IR}$ out of interaction with cTnC. This would be expected to slow relaxation kinetics. Furthermore, the R146G dependent slowdown may also have been due to weaker and thus slower $cTnI_{IR}$ interaction chemistry due to replacement of arginine with glycine. R163W, which produced similar effects to R146G with the exception of a reduced 167C↔89C proximity relative to R146G in the Ca^{2+} and Ca^{2+} + S1-ADP biochemical states (Table 3), did not slow the rate of return of the $cTnI_{IR}$ to actin as much as R146G (Table 4). However, it seemed to slow more the dissociation of the $cTnI_{RR}$ from N-cTnC as suggested by changes in the 167C↔89C distance. Thus once again, kinetic data affirmed that apparently similar mutation-specific physiological effects stem from unique changes to C-cTnI structural behavior and associated impacts on contractility. Importantly, kinetic data matched well with conclusions drawn from changes in FRET efficiency and the steady Ca^{2+} dependence of C-cTnI conformational transitions. But how might the in vitro observations made thus far in the study translate to the physiological setting?

In vitro structural behavior of C-cTnI explains mutation specific changes to skinned fiber behavior

Since the study was done in vitro up to this point, it was reasoned very important to compare structural insights into the mutation specific effects of R146G/Q and R163W on C-cTnI behavior with mutation-specific impacts on at least in situ myocardial contractility. Thus whole cTn complexes reconstituted from cTnC(wt), single-cysteine cTnI mutants containing $S151C_{AEDENS}$, and cTnT(wt) were exchanged into detergent skinned myocardial fibers from rat. Analysis of Western blotting results demonstrated that our exchange efficiency was ≥90% (Fig. 5). Table 5 shows the descriptions of the force-Ca^{2+} relationships of these fibers based on the Hill equation (Eqn. 5). It can be seen that no mutation-specific effects on maximal tension were observed. This was expected, since none of the mutations should produce any effect that would limit the formation of strong XBs within the thin filament. However, in fibers containing R146G passive tension was increased by about 11% of the Ca^{2+} dependent force that was developed by control fibers. This level of additional passive force was tripled in the presence of R146Q, with R163W only slightly less than R146Q. Thus all mutations produced some level of disruption of the $cTnI_{IR}$–actin interaction in situ with R146Q and R163W being more severe, as predicted by prior measurements of FRET efficiency and observations about the effects of S1-ADP on C-cTnI structure in the presence of mutation.

In vitro insights into the effect of mutation on the Ca^{2+}-sensitizing effect of $cTnI_{RR}$ on N-cTnC also proved reliable in situ. R146G and R163W significantly increased the pCa_{50} of the force Ca^{2+} relationship ($p < 0.001$), whereas R146Q actually reduced the pCa_{50} by 0.10 pCa units ($p < 0.001$). This made sense, as both R146G and R163W were expected to enhance the Ca^{2+}-sensitizing $cTnI_{RR}$–cTnC interaction in some way, whereas R146Q was expected to disrupt it. It is notable that only R146G and R163W, which resulted in significantly enhanced Ca^{2+} sensitivity, also resulted in significantly reduced n_H values which implies attenuated cooperativity. Interestingly, this may suggest that $cTnI_{RR}$ mediated Ca^{2+} sensitization of N-cTnC is involved in effecting the apparent cooperativity of Ca^{2+} dependent thin filament regulation. If true, this also implies that the effects of strong XBs on cooperativity [56] may be exerted through their stabilizing effect on the $cTnI_{RR}$–actin interaction [57]. These in situ based insights cemented the in vitro validation of our hypothesis: that R146G/Q and R163W lead to HCM through unique effects on the function of $cTnI_{IR}$, $cTnI_{RR}$, and $cTnI_{MD}$. And these effects were shown to either involve slowing of relaxation, enhancement of the $cTnI_{RR}$–cTnC interaction, and/or disruption of the $cTnI_{IR}$–actin interaction.

DISCUSSION

The present study set out to answer the question of how three different mutations could all lead to HCM, hypothesizing that mutation specific effects arise from unique changes in the structure and function of $cTnI_{IR}$, $cTnI_{RR}$, and $cTnI_{MD}$ during regulatory switching. Investigation was based on the use of FRET as a spectroscopic ruler to provide detailed structural information on the effects of mutation. It was found that both disruption of the $cTnI_{IR}$–actin interaction (seen especially in R146Q and R163W) and enhancement of $cTnI_{RR}$ mediated Ca^{2+} sensitization of cTnC (seen especially in R146G and R163W) were the primary pathways that led to the enhanced Ca^{2+} sensitivity and/or impaired diastolic function that may characterize HCM. Interestingly, the fly casting mechanism was conceptually preserved in spite of mutation, albeit with apparent mutation specific changes to rates of conformational transitions involving the $cTnI_{MD}$, $cTnI_{RR}$, and $cTnI_{IR}$. This underscored the importance of fly casting to relaxation, as well as the connection between conformational equilibria and the dynamic behavior of the sarcomere. All of our experiments also suggested that HCM related mutations may place the TF in a pre relax like

state in the absence of S1-ADP. Finally, in situ measurements of mutation specific effects on the force-Ca^{2+} relationship of detergent-skinned rat myocardium corroborated the insights gained from our in vitro investigations, suggesting that FRET based structural information on regulatory protein function in thin filaments reconstituted in vitro may be predictive of ultimate physiological behavior. Importantly, a linkage was suggested between the Ca^{2+} sensitizing action of $cTnI_{RR}$ on N-cTnC and cooperativity.

To further solidify the promising and biomedically relevant connections between in vitro and in situ measurements seen in our study, more work is needed. Though our steady-state in situ measurements demonstrated consistency between mutation specific effects of R146G/Q and R163W on the Ca^{2+} dependent function of in vitro reconstituted thin filaments and detergent skinned fibers, they did not measure in situ structural changes through FRET. This begs the question of how in situ sarcomeric molecular constraints may affect the conformational transitions of the $cTnI_{IR}$, $cTnI_{RR}$, and $cTnI_{MD}$ relative to in vitro. Some differences may be reasonably expected since the Ca^{2+} affinity of the thin filament in the sarcomeric environment was conservatively ~8.5× less. Though cTnC($S89C_{DDPM}$) may easily be exchanged into our fibers along with our single cysteine cTnI mutants containing $S151C_{AEDENS}$ or $S167C_{AEDENS}$, it would be difficult to determine changes in FRET efficiency through measurement of fluorescence intensity alone. For example, any difference in the extent of protein exchange from fiber to fiber could produce significant error in the measurement. A better method would be to adapt a muscle fiber testing apparatus to perform in situ fluorescence lifetime measurements, since fluorescence lifetimes are independent of fluorophore concentration. Work is currently underway in our laboratory to pursue this goal.

It should also be noted that some differences regarding the in situ effects of R146Q and R163W were obtained compared to the prior study of Takahashi-Yanaga et al. [15]. Particularly, their observations about mutation specific effects on passive tension were somewhat different, as they observed an increase in pCa_{50} due to R145Q and saw less of an enhancement of pCa_{50} by R162W. They also found that R162W reduces the affinity of cTnI for cTnC. However, our data would be more consistent with the notion that R163W (or rather human cTnI(R162W)) increases the affinity of cTnI for cTnC [58]. However, in their investigation human cTnI isoforms containing R145G/Q or R162W were exchanged via whole cTn complexes into rabbit cardiac muscle using a somewhat different protein exchange method. Thus it could be that the differences seen were due to our use of rat cTnI isoforms containing murine analogs of R145G/Q and R162W, or possibly our use of slightly different experimental protocols. Nevertheless, there is good general agreement between our findings and prior work [12–15], especially regarding the effects of R146G.

One important question that could not be answered from the data presented in our study was the significance of some of the more surprising FRET efficiency changes. For example, why was the 167C↔89C proximity decreased relative to control in the presence of R163W and Ca^{2+} (Table 3)? One might expect the 167C↔89C proximity to be increased instead, especially since this was true for the 151C↔89C proximity (Table 2). Also, the disrupted blocked state (i.e. Ca^{2+} and S1-ADP absent) was associated with increases in the 151C↔89C distances relative to control, which almost looked like a tighter interaction with actin that pulled Cys-151 of cTnI further away from Cys-89 of cTnC. However, the 167C↔89C distance in this case was decreased relative to control, suggesting that the $cTnI_{RR}$ was less restricted by $cTnI_{IR}$. So is it possible that Cys-151 of cTnI could move further away from Cys-89C of cTnC in the course of a weaker interaction with actin? Similarly, could Cys-167 of cTnI actually move further away from Cys-89C in the process of $cTnI_{RR}$ forming a tighter interaction with cTnC? One way to answer these questions experimentally is to investigate FRETs between cTnI($S151C_{AEDENS}$) or

cTnI(S167C_{AEDENS}) and actin(374C_{DDPM}) as we have performed previously [40, 59], but in the presence of mutations. Based on how Cys-167 or Cys-151 of cTnI become either closer to or distant from Cys-374 of actin, the questions raised from close inspection of Tables 2 and 3 could be answered. One challenge to this approach would be reliably incorporating fluorescently labeled actin into in situ thin filaments.

In conclusion, Nature has produced a remarkably fine tuned, precisely calibrated, and perfectly balanced molecular mechanism in the regulatory switching action of cTn in which C-cTnI plays an essential role. Our study suggests that R146G/Q and R163W lead to HCM because they disrupt C-cTnI functional regions enough to disturb Nature's balance, but not so well that the molecular mechanism itself is conceptually changed. In other words, R146G/Q and R163W result in HCM particularly because these mutations merely tweak the way that the functional regions of C-cTnI behave without fundamentally changing the drag and release or fly casting mechanisms or completely abolishing C-cTnI mediated inhibition of the XB cycle. Nevertheless, physiological demand for tightly controlled, adaptable, and constantly functioning cardiac pumping makes these tweaks highly problematic to the survival of an HCM afflicted organism. In fact, these HCM related mutations may cause the TF to approximate the pre relax state in the absence of crossbridge formation, disturbing the balance between possible conformational states that is necessary to reliable function. What is unsettling about our data is that R146G/Q and R163W achieve similar ultimate effects through entirely different means. Our data thus suggest that different HCM related mutations, and perhaps all cardiomyopathy mutations, may not only exert unique mutation specific effects, but may also require mutation specific advances in treatment if cures are to ever be realized.

Acknowledgments

We would like to thank Murali Chandra and his laboratory for the kind gift of N-terminal myc-tagged cTnT and for providing guidance concerning cTn exchange and muscle fiber testing. We are also very grateful to Jaak Panksepp for generously providing Long-Evans rats used for in situ measurements and Sheri Six of the Panskepp lab for assistance with animal handling protocols. This work was supported by National Institute of Health Grants HL80186 and HL80186-5S1 (to W.-J. D.), as well as the M.J. Murdock Charitable Trust (to W.-J. D.).

REFERENCES

[1]. Maron BJ, Bonow RO, Cannon RO 3rd, Leon MB, Epstein SE. New Engl. J. Med. 1987; 316:780–789. [PubMed: 3547130]

[2]. Maron BJ, McKenna WJ, Danielson GK, Kappenberger LJ, Kuhn HJ, Seidman CE, Shah PM, Spencer WH 3rd, Spirito P, Ten Cate FJ, Wigle ED. J. Am. Coll. Cardiol. 2003; 42:1687–1713. [PubMed: 14607462]

[3]. Seidman JG, Seidman C. Cell. 2001; 104:557–567. [PubMed: 11239412]

[4]. Fatkin D, McConnell BK, Mudd JO, Semsarian C, Moskowitz IG, Schoen FJ, Giewat M, Seidman CE, Seidman JG. J. Clin. Invest. 2000; 106:1351–1359. [PubMed: 11104788]

[5]. Gomes AV, Potter JD. Mol. Cell. Biochem. 2004; 263:99–114. [PubMed: 15524171]

[6]. Kimura A, Harada H, Park JE, Nishi H, Satoh M, Takahashi M, Hiroi S, Sasaoka T, Ohbuchi N, Nakamura T, Koyanagi T, Hwang TH, Choo JA, Chung KS, Hasegawa A, Nagai R, Okazaki O, Nakamura H, Matsuzaki M, Sakamoto T, Toshima H, Koga Y, Imaizumi T, Sasazuki T. Nat. Genet. 1997; 16:379–382. [PubMed: 9241277]

[7]. Van Driest SL, Ellsworth EG, Ommen SR, Tajik AJ, Gersh BJ, Ackerman MJ. Circulation. 2003; 108:445–451. [PubMed: 12860912]

[8]. Niimura H, Patton KK, McKenna WJ, Soults J, Maron BJ, Seidman JG, Seidman CE. Circulation. 2002; 105:446–451. [PubMed: 11815426]

[9]. Richard P, Charron P, Carrier L, Ledeuil C, Cheav T, Pichereau C, Benaiche A, Isnard R, Dubourg O, Burban M, Gueffet JP, Millaire A, Desnos M, Schwartz K, Hainque B, Komajda M. Circulation. 2003; 107:2227–2232. [PubMed: 12707239]

[10]. Kokado H, Shimizu M, Yoshio H, Ino H, Okeie K, Emoto Y, Matsuyama T, Yamaguchi M, Yasuda T, Fujino N, Ito H, Mabuchi H. Circulation. 2000; 102:663–669. [PubMed: 10931807]

[11]. Morner S, Richard P, Kazzam E, Hainque B, Schwartz K, Waldenstrom A. J. Mol. Cell. Cardiol. 2000; 32:521–525. [PubMed: 10731450]

[12]. Takahashi-Yanaga F, Morimoto S, Ohtsuki I. J. Biol. Chem. 2000; 127:355–357.

[13]. Lang R, Gomes AV, Zhao J, Housmans PR, Miller T, Potter JD. J. Biol. Chem. 2002; 277:11670–11678. [PubMed: 11801593]

[14]. Wen Y, Pinto JR, Gomes AV, Xu Y, Wang Y, Potter JD, Kerrick WG. J. Biol. Chem. 2008; 283:20484–20494. [PubMed: 18430738]

[15]. Takahashi-Yanaga F, Morimoto S, Harada K, Minakami R, Shiraishi F, Ohta M, Lu QW, Sasaguri T, Ohtsuki I. J. Mol. Cell. Cardiol. 2001; 33:2095–2107. [PubMed: 11735257]

[16]. Geeves MA, Chai M, Lehrer SS. Biochem. 2000; 39:9345–9350. [PubMed: 10924128]

[17]. Murakami K, Yumoto F, Ohki SY, Yasunaga T, Tanokura M, Wakabayashi T. J. Mol. Biol. 2005; 352:178–201. [PubMed: 16061251]

[18]. Blumenschein TM, Stone DB, Fletterick RJ, Mendelson RA, Sykes BD. Biophys. J. 2006; 90:2436–2444. [PubMed: 16415057]

[19]. Galinska A, Hatch V, Craig R, Murphy AM, Van Eyk JE, Wang CL, Lehman W, Foster DB. Circ. Res. 2010; 106:705–711. [PubMed: 20035081]

[20]. Galinska-Rakoczy A, Engel P, Xu C, Jung H, Craig R, Tobacman LS, Lehman W. J. Mol. Biol. 2008; 379:929–935. [PubMed: 18514658]

[21]. Lehman W, Galinska-Rakoczy A, Hatch V, Tobacman LS, Craig R. J. Mol. Biol. 2009; 388:673–681. [PubMed: 19341744]

[22]. Haselgrove JC. Cold Spring Harbor Symp. Qant. Biol. 1972; 37:341–352.

[23]. Huxley HE. Cold Spring Harbor Symp. Quant. Biol. 1973; 37:361–376.

[24]. Parry DA, Squire JM. J. Mol. Biol. 1973; 75:33–55. [PubMed: 4713300]

[25]. Dong WJ, Xing J, Villain M, Hellinger M, Robinson JM, Chandra M, Solaro RJ, Umeda PK, Cheung HC. J. Biol. Chem. 1999; 274:31382–31390. [PubMed: 10531339]

[26]. Li MX, Spyracopoulos L, Sykes BD. Biochem. 1999; 38:8289–8298. [PubMed: 10387074]

[27]. Dong WJ, Cheung HC. Biochim. Biophys. Acta. 1996; 1295:139–146. [PubMed: 8695639]

[28]. Perry SV. Mol. Cell Biochem. 1999; 190:9–32. [PubMed: 10098965]

[29]. Robinson JM, Dong WJ, Xing J, Cheung HC. J. Mol. Biol. 2004; 340:295–305. [PubMed: 15201053]

[30]. Kobayashi T, Solaro RJ. Annu. Rev. Physiol. 2005; 67:39–67. [PubMed: 15709952]

[31]. Li MX, Wang X, Sykes BD. J. Muscle Res. Cell. Motil. 2004; 25:559–579. [PubMed: 15711886]

[32]. Hoffman RM, Blumenschein TM, Sykes BD. J. Mol. Biol. 2006; 361:625–633. [PubMed: 16876196]

[33]. Zhou Z, Li KL, Rieck D, Ouyang Y, Chandra M, Dong WJ. J. Biol. Chem. 287:7661–7674. [PubMed: 22207765]

[34]. Zhou X, Morris EP, Lehrer SS. Biochem. 2000; 39:1128–1132. [PubMed: 10653659]

[35]. Mudalige WA, Tao TC, Lehrer SS. J. Mol. Biol. 2009; 389:575–583. [PubMed: 19379756]

[36]. Lehrer SS. J. Muscle Res. Cell. Motil. 2011; 32:203–208. [PubMed: 21948173]

[37]. Vinogradova MV, Stone DB, Malanina GG, Karatzaferi C, Cooke R, Mendelson RA, Fletterick RJ. Proc Natl Acad Sci U S A. 2005; 102:5038–5043. [PubMed: 15784741]

[38]. Takeda S, Yamashita A, Maeda K, Maeda Y. Nature. 2003; 424:35–41. [PubMed: 12840750]

[39]. Dong WJ, Xing J, Ouyang Y, An J, Cheung HC. J. Biol. Chem. 2008; 283:3424–3432. [PubMed: 18063575]

[40]. Xing J, Jayasundar JJ, Ouyang Y, Dong WJ. J. Biol. Chem. 2009; 284:16432–16441. [PubMed: 19369252]

[41]. Dong WJ, Chandra M, Xing J, Solaro RJ, Cheung HC. Biochem. 1997; 36:6745–6753. [PubMed: 9184156]

[42]. Dong WJ, Xing J, Robinson JM, Cheung HC. J. Mol. Biol. 2001; 314:51–61. [PubMed: 11724531]

[43]. Dong WJ, Robinson JM, Stagg S, Xing J, Cheung HC. J. Biol. Chem. 2003; 278:8686–8692. [PubMed: 12511564]

[44]. Smillie LB. Meth. Enzymol. 1982; 85:234–241. [PubMed: 6289041]

[45]. Xing J, Cheung HC. Arch. Biochem. Biophys. 1994; 313:229–234. [PubMed: 8080266]

[46]. Pardee JD, Spudich JA. Meth. Enzymol. 1982; 85:164–181. [PubMed: 7121269]

[47]. Liao R, Wang CK, Cheung HC. Biophys. J. 1992; 63:986–995. [PubMed: 1420937]

[48]. Dong WJ, Robinson JM, Xing J, Cheung HC. J. Biol. Chem. 2003; 278:42394–42402. [PubMed: 12909617]

[49]. Chandra M, Tschirgi ML, Rajapakse I, Campbell KB. Biophys. J. 2006; 90:2867–2876. [PubMed: 16443664]

[50]. de Tombe PP, Belus A, Piroddi N, Scellini B, Walker JS, Martin AF, Tesi C, Poggesi C. Am. J. Physiol. Regul. Integr. Comp. Physiol. 2007; 292:R1129–1136. [PubMed: 17082350]

[51]. Chandra M, Tschirgi ML, Ford SJ, Slinker BK, Campbell KB. Am. J. Physiol. Regul. Integr. Comp. Physiol. 2007; 293:R1595–1607. [PubMed: 17626127]

[52]. Guth K, Wojciechowski R. Pflugers Arch. 1986; 407:552–557. [PubMed: 2947040]

[53]. Dweck D, Reyes-Alfonso A Jr. Potter JD. Anal. Biochem. 2005; 347:303–315. [PubMed: 16289079]

[54]. Solaro RJ. J. Physiol. 2009; 587:3. [PubMed: 19119179]

[55]. Piper HM, Abdallah Y, Schafer C. Cardiovasc. Res. 2004; 61:365–371. [PubMed: 14962469]

[56]. Moss RL, Razumova M, Fitzsimons DP. Circ. Res. 2004; 94:1290–1300. [PubMed: 15166116]

[57]. Sun YB, Irving M. J. Mol. Cell. Cardiol. 2010; 48:859–865. [PubMed: 20004664]

[58]. Elliott K, Watkins H, Redwood CS. J. Biol. Chem. 2000; 275:22069–22074. [PubMed: 10806205]

[59]. Xing J, Chinnaraj M, Zhang Z, Cheung HC, Dong WJ. Biochem. 2008; 47:13383–13393. [PubMed: 19053249]

HIGHLIGHTS

- FRET study of effects of HCM-related cTnI mutations in reconstituted thin filaments
- R146G/Q and R163W each uniquely impact interactions between cTnI and cTnC or actin
- Fly casting mechanism underlying deactivation preserved in spite of mutation
- R146G/Q and R163W cause TF to enter pre relax like state in the absence of S1-ADP
- In situ effects on force–Ca^{2+} relationship of myocardial fibers matches in vitro

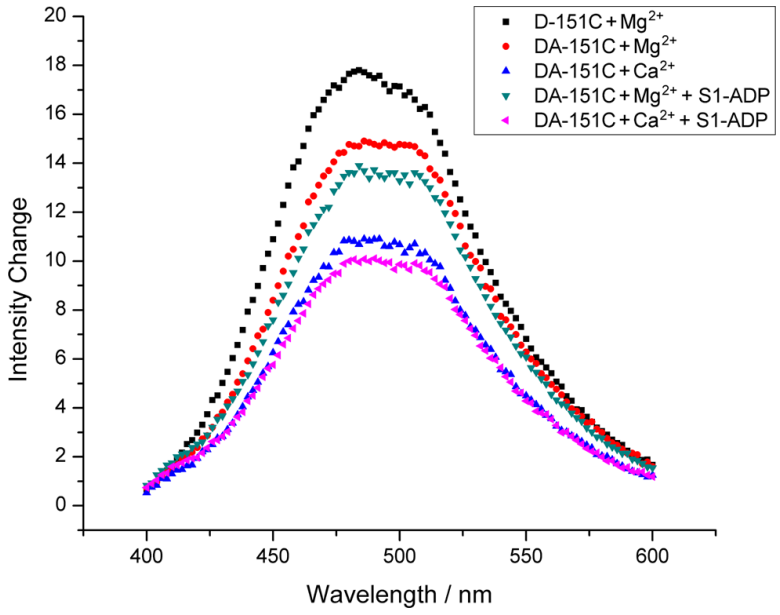

Figure 1.

Representative traces of biochemically induced changes in AEDANS emission spectral intensity as observed in reconstituted thin filaments containing cTnI(S151C$_{AEDENS}$) and either cTnC(S89C$_{DDPM}$) or cTnC(wt). Note that in the legend, “D-151C” indicates donor only samples that contain cTnI(S151C$_{AEDENS}$) and cTnC(wt), whereas “DA-151C” denotes samples containing cTnI(S151C$_{AEDENS}$) and cTnC(S89C$_{DDPM}$).

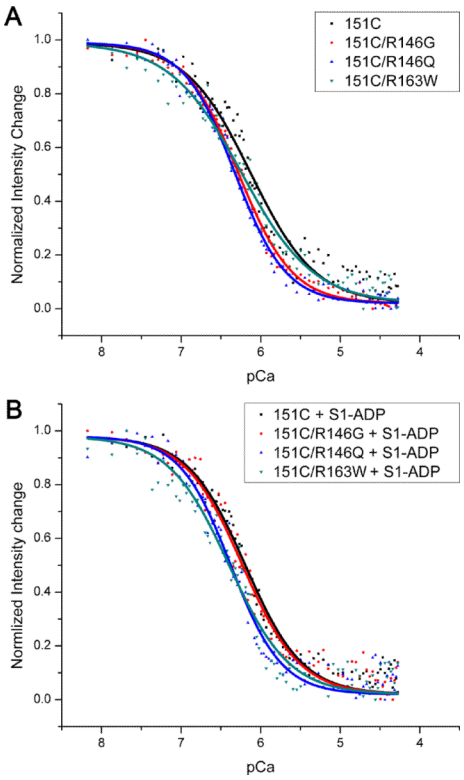

Figure 2.

Fluorescence intensity changes due to changes in FRET during Ca^{2+} titrations in the presence/absence of S1 performed on cardiac thin filaments reconstituted with $cTnC(89C)_{DDPM}$ and single cysteine cTnI mutants containing $S151C_{AEDENS}$.

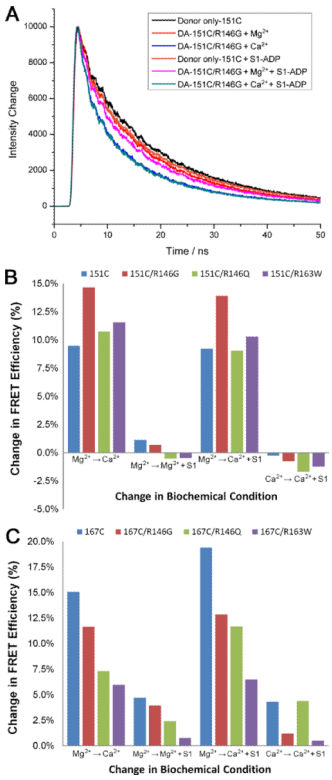

Figure 3.

Use of fluorescence lifetime measurements to accurately determine FRET efficiency as a function of mutation state and biochemical condition. (A) Fluorescence intensity decays of thin filaments reconstituted with cTnC($S89C_{DDPM}$) and single cysteine cTnI mutants containing $S151C_{AEDENS}$. (B) Changes in FRET efficiency between $S89C_{DDPM}$ of cTnC and $S151C_{AEDENS}$ of cTnI due to changes in biochemical conditions. (C) Changes in FRET efficiency between $S89C_{DDPM}$ of cTnC and $S167C_{AEDENS}$ of cTnI due to changes in biochemical conditions.

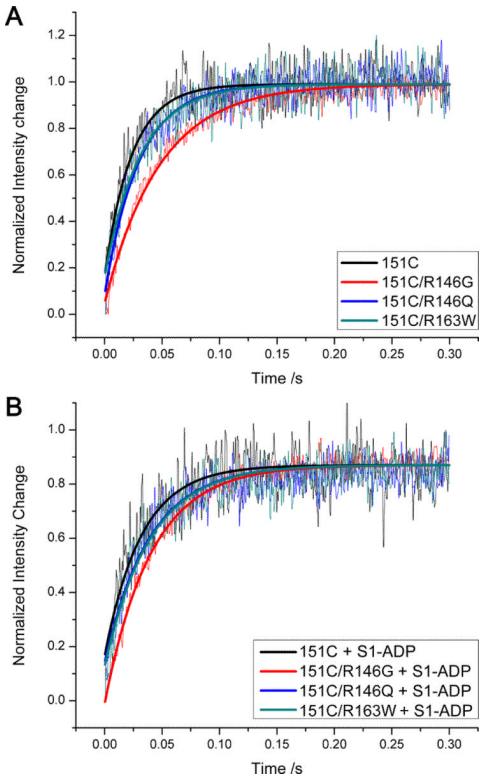

Figure 4.

Ca^{2+}-dissociation induced stopped-flow kinetics of cardiac thin filaments reconstituted with $cTnC(89C)_{DDPM}$ and single cysteine cTnI mutants containing $S151C_{AEDENS}$.

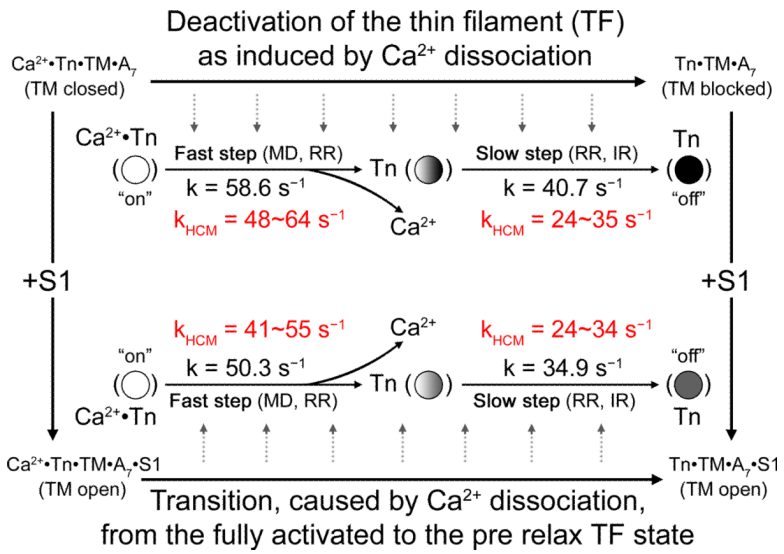

Scheme 1.

A diagram of the specific effects of HCM related cTnI mutations R146/Q and R163W on the kinetics of regional structural transitions involved in TF deactivation.

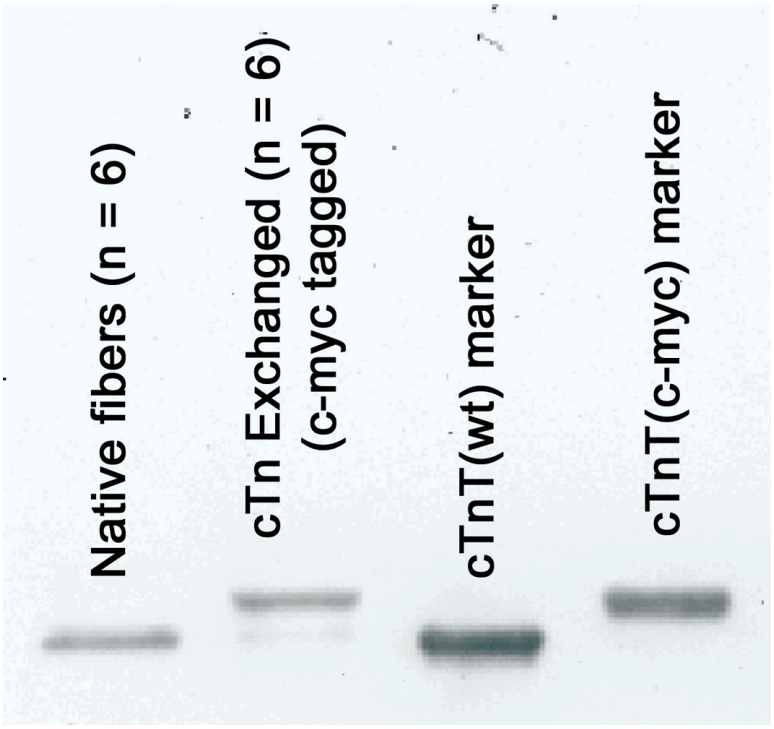

Figure 5.

A representative gel depicting the effectiveness of our cTn exchange protocol. In this example, cTn complexes reconstituted with cTnC(wt), cTnI(wt), and N-terminal myc tagged cTnT were exchanged into native fibers. Protein bands were visualized using antibody against cTnT. It is evident from the Western blot that nearly complete exchange was accomplished.

Table 1

Steady state Ca^{2+} dependence of changes in FRET, as described by the Hill equation (Eqn. 1), observed in reconstituted cardiac thin filaments containing cTnC(S89C_{DDPM}) and either cTnI(S151C_{AEDENS}) or cTnI(S167C_{AEDENS}).

cTnI mutants (n = 5)	Thin filament		Thin filament + S1-ADP	
	pCa_{50}	n_H	pCa_{50}	n_H
151C	6.12 ± 0.02	1.53 ± 0.04	6.22 ± 0.02[d]	1.20 ± 0.04[d]
151C/R146G	6.26 ± 0.01[a]	1.39 ± 0.04[a]	6.28 ± 0.02[b]	1.20 ± 0.05[d]
151C/R146Q	6.31 ± 0.01[a]	1.48 ± 0.05	6.42 ± 0.02[a,d]	1.36 ± 0.05[a,e]
151C/R163W	6.21 ± 0.02[a]	1.22 ± 0.07[a]	6.45 ± 0.02[a,d]	1.14 ± 0.06
167C	6.14 ± 0.02	1.53 ± 0.07	6.32 ± 0.07[d]	1.34 ± 0.06[e]
167C/R146G	6.48 ± 0.02[a]	1.37 ± 0.06[b]	6.53 ± 0.06[a]	1.24 ± 0.17
167C/R146Q	6.23 ± 0.02[a]	1.25 ± 0.06[a]	6.28 ± 0.07	1.54 ± 0.15[c,e]
167C/R163W	6.41 ± 0.03[a]	1.18 ± 0.10[a]	6.59 ± 0.03[a,d]	1.12 ± 0.07[a]

[a] A mutation specific effect on either the pCa_{50} or n_H describing steady state and Ca^{2+} dependent changes in FRET efficiency was observed with $p < 0.001$,

[b] $p < 0.01$, or

[c] $p < 0.05$.

[d] The addition of S1 significantly affected either the pCa_{50} or n_H of changes in FRET with $p < 0.001$,

[e] $p < 0.01$, or

[f] $p < 0.05$.

Table 2

Ca^{2+}- and S1-dependent changes in AEDENS fluorescence lifetime and FRET efficiency due to distance changes between $S151C_{AEDENS}$ of cTnI and $S89C_{DDPM}$ of cTnC in reconstituted cardiac thin filaments.

cTnI samples[a]	Thin filament + Mg^{2+}				Thin filament + S1-ADP + Mg^{2+}			
	τ_1[b]/α_1	τ_2[b]/α_2	$\bar{\tau}_{DA}$ [b]	E[c]	ϕ_1/α_1	ϕ_2/α_2	$\bar{\tau}_{DA}$	E[d]
151C	2.51/0.09	14.11/0.91	13.07	15.46%	2.13/0.12	13.94/0.88	12.52	16.59%
151C/R146G	2.52/0.08	14.49/0.92	13.53	12.44%	2.34/0.10	14.23/0.90	13.04	13.14%[f]
151C/R146Q	2.69/0.08	14.27/0.92	13.34	13.66%	2.62/0.10	14.20/0.90	13.04	13.14%[f]
151C/R163W	2.70/0.11	14.45/0.89	13.16	14.87%[e]	2.61/0.12	14.25/0.88	12.85	14.39%[f]
	Thin filament + Ca^{2+}				Thin filament + S1-ADP + Ca^{2+}			
	τ_1/α_1	τ_2/α_2	$\bar{\tau}_{DA}$	E[c]	τ_1/α_1	τ_2/α_2	$\bar{\tau}_{DA}$	E[d]
151C	2.37/0.15	13.31/0.85	11.67	24.95%	2.38/0.18	13.34/0.82	11.37	24.68%[g]
151C/R146G	2.21/0.16	13.07/0.84	11.33	27.11%	2.11/0.16	12.83/0.84	11.11	26.35%[g]
151C/R146Q	2.42/0.14	13.27/0.86	11.75	24.42%[e]	2.44/0.16	13.42/0.84	11.66	22.72%
151C/R163W	2.42/0.16	13.16/0.84	11.44	26.41%	2.38/0.17	13.12/0.83	11.29	25.17%

[a] For each sample category, n = 5.

[b] The units of τ_1 τ_2, and $\bar{\tau}_{DA}$ are ns. The standard deviation of the reported lifetimes throughout the table ranged from ±0.04 ns to ±0.08 ns.

[c] FRET efficiency was calculated from Eqn. 4 by comparing donor-acceptor samples to donor only samples. In the absence of Ca^{2+}, $\bar{\tau}_D$ = 15.46 ± 0.04 ns. In the presence of Ca^{2+}, $\bar{\tau}_D$ = 15.55 ± 0.04 ns. The standard deviation of calculated FRET efficiencies reportedhere ranged from ±0.49% to ±0.59%.

[d] In the absence of Ca^{2+} and with S1 present, $\bar{\tau}_D$ = 15.01 ± 0.04 ns. In the presence of Ca^{2+} and with S1 present, $\bar{\tau}_D$ = 15.09 ± 0.04 ns. The standard deviation of calculated FRET efficiencies reported here ranged from ±0.51% to ±0.59%.

[e] No mutation-specific change in FRET efficiency was observed ($p > 0.05$) under this biochemical condition.

[f] The addition of S1 in the absence of Ca^{2+} did not produce a statistically significant change FRET efficiency ($p > 0.05$).

[g] The addition of S1 in the presence of Ca^{2+} did not significantly change the FRET efficiency ($p > 0.05$).

Table 3

Ca^{2+}- and S1-dependent changes in AEDENS fluorescence lifetime and FRET efficiency due to distance changes between $S167C_{AEDENS}$ of cTnI and $S89C_{DDPM}$ of cTnC in reconstituted cardiac thin filaments.

cTnI samples[a]	Thin filament + Mg^{2+}				Thin filament + S1-ADP + Mg^{2+}			
	$\tau_1[b]/\alpha_1$	$\tau_2[b]/\alpha_2$	$\bar{\tau}_{DA}$ [b]	E[c]	τ_1/α_1	τ_2/α_2	$\bar{\tau}_{DA}$	E[d]
167C	1.79/0.05	15.27/0.95	14.64	2.97%	1.36/0.06	14.46/0.94	13.69	7.68%
167C/R146G	2.11/0.06	14.46/0.94	13.71	9.18%	1.86/0.07	13.76/0.93	12.88	13.14%
167C/R146Q	2.31/0.05	15.02/0.95	14.42	4.43%	1.83/0.05	14.52/0.95	13.81	6.85%
167C/R163W	1.46/0.07	14.82/0.93	13.84	8.33%	1.28/0.08	14.55/0.92	13.48	9.11%[e]
	Thin filament + Ca^{2+}				Thin filament + S1-ADP + Ca^{2+}			
	τ_1/α_1	τ_2/α_2	$\bar{\tau}_{DA}$	E[c]	τ_1/α_1	τ_2/α_2	$\bar{\tau}_{DA}$	E[d]
167C	2.07/0.10	13.36/0.90	12.29	18.05%	1.54/0.10	12.66/0.90	11.56	22.37%
167C/R146G	2.11/0.10	12.90/0.90	11.87	20.83%	1.81/0.09	12.63/0.91	11.61	22.04%[f]
167C/R146Q	2.41/0.08	14.12/0.92	13.24	11.74%	1.31/0.10	13.70/0.90	12.49	16.12%
167C/R163W	1.50/0.10	14.06/0.90	12.85	14.32%	1.35/0.11	13.99/0.89	12.68	14.84%[g]

[a] For each sample category, n = 5.

[b] The units of $\phi 1$, $\phi 2$, and $\bar{\phi}_{DA}$ are ns. The standard deviation of the reported lifetimes throughout the table ranged from ±0.03 ns to ±0.11 ns.

[c] FRET efficiency was calculated from Eqn. 4 by comparing donor-acceptor samples to donor only samples. In the absence of Ca^{2+}, $\bar{\phi}_D$ = 15.09 ± 0.06 ns. In the presence of Ca^{2+}, $\bar{\phi}_D$ = 15.00 ± 0.05 ns. The standard deviation of calculated FRET efficiencies reportedhere ranged from ±0.51% to ±0.64%.

[d] In the absence of Ca^{2+} and with S1 present, $\bar{\phi}_D$ = 14.83 ± 0.04 ns. In the presence of Ca^{2+} and with S1 present, $\bar{\phi}_D$ = 14.89 ± 0.04 ns. The standard deviation of calculated FRET efficiencies reported here ranged from ±0.43% to ±0.59%.

[e] The addition of S1 in the absence of Ca^{2+} did not produce a statistically significant change FRET efficiency ($p > 0.05$).

[f] No mutation-specific change in FRET efficiency was observed ($p > 0.10$) under this biochemical condition.

[g] The addition of S1 in the presence of Ca^{2+} did not significantly change the FRET efficiency ($p > 0.10$).

Table 4

Kinetics of changes in FRET efficiency induced by Ca^{2+} dissociation and observed in cardiac thin filaments reconstituted with cTnC($S89C_{DDPM}$) and single cysteine cTnI mutants containing either $S151C_{AEDENS}$ or $S167C_{AEDENS}$.

cTnI mutants	Kinetic rate/ s^{-1}	
	Thin filament	Thin filament +S1-ADP
151C	40.7 ± 1.3	34.9 ± 1.3[d]
151C/R146G	23.6 ± 0.2[a]	23.5 ± 0.2[a]
151C/R146Q	34.9 ± 0.8[a]	33.7 ± 0.8[f]
151C/R163W	33.3 ± 1.0[a]	31.2 ± 0.7[a,e]
167C	58.6 ± 1.5	50.3 ± 2.2[d]
167C/R146G	49.6 ± 0.9[a]	46.6 ± 1.1[b,e]
167C/R146Q	63.7 ± 2.1[b]	54.5 ± 3.3[c,d]
167C/R163W	47.7 ± 1.3[a]	40.7 ± 0.7[a,d]

[a] A mutation specific effect on the kinetics of changes in FRET efficiency was observed with $p < 0.001$,

[b] $p < 0.01$, or

[c] $p < 0.05$.

[d] The addition of S1 affected the kinetics of changes in FRET efficiency with $p < 0.001$,

[e] $p < 0.01$, or

[f] $p < 0.05$.

Table 5

Properties of detergent skinned fiber bundles that have undergone protein exchange during incubation with cTn complexes reconstituted from cTnC(wt), cTnT(wt), and single cysteine cTnI mutants containing $S151C_{AEDENS}$

cTnI mutant (n = 5)	Tension *(mN/mm²)*		pCa_{50}	n_H
	Maximum	**Passive**		
$S151C_{AEDENS}$	35.85 ± 3.58	3.05 ± 0.70	5.39 ± 0.03	2.22 ± 0.42
$S151C_{AEDENS}$/R146G	35.29 ± 2.78	6.62 ± 0.81[a]	5.51 ± 0.02[a]	1.61 ± 0.22[c]
$S151C_{AEDENS}$/R146Q	34.84 ± 1.85	14.03 ± 2.76[a]	5.29 ± 0.03[a]	2.02 ± 0.31
$S151C_{AEDENS}$/R163W	33.23 ± 1.16	12.39 ± 0.41[a]	5.54 ± 0.02[a]	1.28 ± 0.13[b]

[a] A mutation specific effect on either the maximum tension, passive tension, pCa_{50} or n_H associated with the force–Ca^{2+} relationship was observed with $p < 0.001$,

[b] $p < 0.01$, or

[c] $p < 0.05$.